



Materials Science

An Indian Journal

Full Paper

MSAIJ, 14(4), 2016 [139-148]

Test of elaboration protocols for obtaining highly Co- or Ni -alloyed spheroidal cast irons from an industrial SG cast iron. Part B: second protocol. subpart 1: obtained microstructures

Kamel Meridja, Patrice Berthod*, Elodie Conrath

Institut Jean Lamour (UMR 7198), Team 206 "Surface and Interface, Chemical Reactivity of Materials" Faculty of Sciences and Technologies, University of Lorraine, B.P. 70239, 54506 Vandoeuvre-lès-Nancy, (FRANCE)

E-mail: Patrice.Berthod@univ-lorraine.fr

ABSTRACT

{Co, Fe}-based and {Ni, Fe}-based cast irons with spheroidal graphite may be interesting alloys, simultaneously easy to cast, displaying high mechanical properties including tensile strength, chromium-free corrosion-resistant... A first protocol tested to obtain such cast irons at a laboratory scale without the liquid metal treatment facilities of industry, did not succeed in obtaining a nodular shape for graphite. In this new work, an elaboration in two steps involving the preparation then the use of mother alloys, was imagined and applied. Graphite spheroids were successfully obtained in the cobalt-rich cast iron, but together with flake graphite. Since the same protocol applied to the elaboration of similar cast iron but with only Fe, in parallel for comparison, allowed recovering the total nodular character of graphite, it seems that nickel, and maybe partially cobalt too, are intrinsically unfavourable to the spheroidal growth of graphite during solidification.

© 2016 Trade Science Inc. - INDIA

KEYWORDS

Spheroidal graphite cast iron;
Nickel;
Cobalt;
Microstructure;
Optical microscopy;
SEM;
XRD.

INTRODUCTION

Cast irons coming from the bottom part of blast furnaces are generally relatively pure liquid Fe-C-Si alloys. Indeed, besides iron (the wished element, brought by ore), carbon (the iron oxide reducing agent, brought by coke) and silicon (resulting from the reduction of the silica present in the iron ore), impurities such as sulphur (S) also exists and perturbs the spheroidal growth of graphite. When this is flake graphite which is wished one must only check that its contents is not too high to avoid the forma-

tion of brittle phases resulting of the combination of Fe and S. In contrast, when good tensile strength and high ductility and toughness are required by the final applications, the spheroidal shape is compulsory and S has to be removed almost totally, by desulfurization of the liquid iron and its magnesium treatment, before being inoculated and poured^[1-7].

Such treatments devoted to the suppression of sulphur, dissolved oxygen and of all poison elements may be difficult to apply in a laboratory to obtain small samples for academic studies for example. Fortunately a test earlier carried out for adding

Full Paper

supplementary silicon to a small part of spheroidal graphite cast iron cut in a piece industrially elaborated demonstrated that the spheroidal shape of graphite can be recovered after re-melting and re-solidification in inert atmosphere, without any supplementary treatment of the molten alloy^[8, 9]. In order to add – not simply a small quantity of silicon – but several tens of weight percents of a new element (Co or Ni), the obtained graphite structure was not at all spheroidal^[10]. It was thought that this was due to the thermal treatment applied to the liquid alloy which was imposed by the difficulty to melt the added elements: Co or Ni, but also supplementary Si and C to do not change their final contents in the new cast iron. The graphite parts which were added to maintain the C content although Co or Ni were added with quantities equals to the Fe of the initial cast iron, took much more time to be incorporated in the melt, furthermore at a temperature which was increased at a very high level. Since the Fe-added cast iron elaborated following the same route for comparison (for a better identification of the specific role of Co and of Ni by excluding the effect of all other possible difference in the elaboration) was itself without spheroidal graphite but with flake one, this was not specifically Co or Ni but also possibly the modified thermal cycle which was responsible to the loss of the spheroidal graphite shape.

In this new work, another protocol was applied, to respect the thermal cycle which earlier allowed recovering the spheroidal shape of graphite^[8, 9]. By excluding the suspected possible effect of overheating, this should permit seeing if spheroidal graphite may be obtained in a so-unusual elaboration route, and to study any possible role of Co and Ni on the obtained graphite shape. Here too a cast iron elaborated following the same new route but with supplementary Fe instead Co or Ni, will be elaborated and metallographically characterized.

EXPERIMENTAL

Elaboration of the alloys

To avoid any overheating in presence of the spheroids of the industrial cast iron the elaboration was carried out with two successive steps. A first elabo-

ration was the one of the added elements together, the SG iron part excluded. A charge of about 20g constituted of pure Co, Si and C (graphite) was separately melted under 400mbars of pure Argon with the same High Frequency Induction furnace of CELES used in the previous work^[10]. After a rather long exposure (10 minutes) at very high temperature (corresponding to the 5kV voltage), almost all the graphite has entered the molten alloy. Solidification led to a 20g-ingot of a {Co-3.5C, 2.5Si} cobalt-mother alloy (chemical composition in wt.%). Two other similar 20g-weighing mother alloys, {Ni-3.5C, 2.5Si} and {Fe-3.5C, 2.5Si}, were obtained following the same route. Thereafter a 20g-weighing part of industrial spheroidal graphite cast iron was re-melted together with the 20g-weighing {Co-3.5C, 2.5Si} mother alloy, the re-melting of which was very easy. The applied heating was realized until reaching 2.5kV. After a 30 seconds stage at 2.5kV, the power was increased up to 3.5kV. After a 30 seconds stage at 3.5kV – what allowed a total melting of the SG iron part and of the mother alloy together and the homogenization of the liquid, the power was decreased until 0, and the solidified ingot cooled rapidly and more and more slowly down to room temperature. Thus, the thermal cycle known by the part of industrial SG iron, was rigorously the same as the one which allowed earlier obtaining a SG cast iron enriched in Si^[8, 9].

Ingots' cutting and samples' machining

The obtained ingots were first immersed in a liquid mix of cold resin system (82% CY230 resin and 18% HY253Hardener closely mixed together) in order to obtain a cylindrical mounted ingot much easier to handle then cut. This one was cut using a Buehler Abrasimet Delta metallographic saw to obtain parts for the metallographic characterization and parallelepipeds devoted to the compression tests.

Metallographic characterization

The parts prepared for the metallographic characterization were imbedded in the same cold resin system as mentioned above, ground with SiC papers whose grade increased from 120 to 4000. After ultrasonic cleaning, polishing was done using a textile disk supplied in 1 μ m alumina or diamond

particles.

The mounted and polished samples were first observed using a Olympus optical microscope (BX51 model) equipped with a digital camera (ToupCam) driven with a software (ToupView), to study the graphite shape. Thereafter a Nital etching was applied to observe the metallic matrix (immersion in an {ethanol-4% HNO₃} etchant for about 10 seconds, at room temperature), using the same microscope.

The same samples were also observed by Scanning Electron Microscopy (SEM) using a JEOL JSM 6010LA apparatus equipped with an Energy Dispersion Spectrometry (EDS) device. This was essentially to control the global chemical compositions of the obtained ingots and to specify the chemical composition of the matrix. However it was verified if more details concerning the matrix were visible, to complete the observations done by optical microscopy.

X-Ray Diffraction characterization of the microstructure was also performed using a Philips X'Pert Pro diffractometer (anticathode of copper, K_α transition of Cu with wavelength: 1.5406 Angströms), and the generated files were analyzed using the EVA software.

RESULTS AND DISCUSSION

Optical microstructure observations

Several micrographs were taken per alloy: two at different magnifications on three distinct zones ("CoFe2" and "NiFe2" alloys only), without any etching. They are displayed in Figure 1 (not etched) and Figure 2 (etched) for the cast iron containing as cobalt as iron (noted "CoFe2"), in Figure 3 (not etched) and Figure 4 (etched) for the cast iron containing as nickel as iron (noted "NiFe2"), and in Figure 5 (not etched) and Figure 6 (etched) for the cast iron containing only iron (noted "FeFe2"). The observations which can be done about the graphite structures and the matrix among the three locations in each alloy are:

"CoFe2" (Co=Fe + 3.5C + 2.5Si):

Before etching (Figure 1): obviously eutectic-

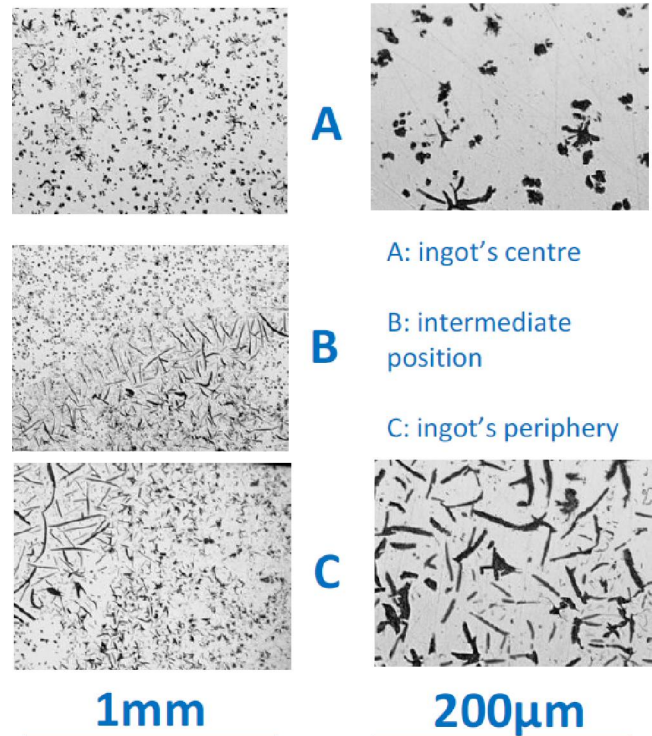


Figure 1 : Graphite structure (without etching) of the "CoFe2" cast iron as observed at two magnifications in three distinct zones ("A", "B" and "C")

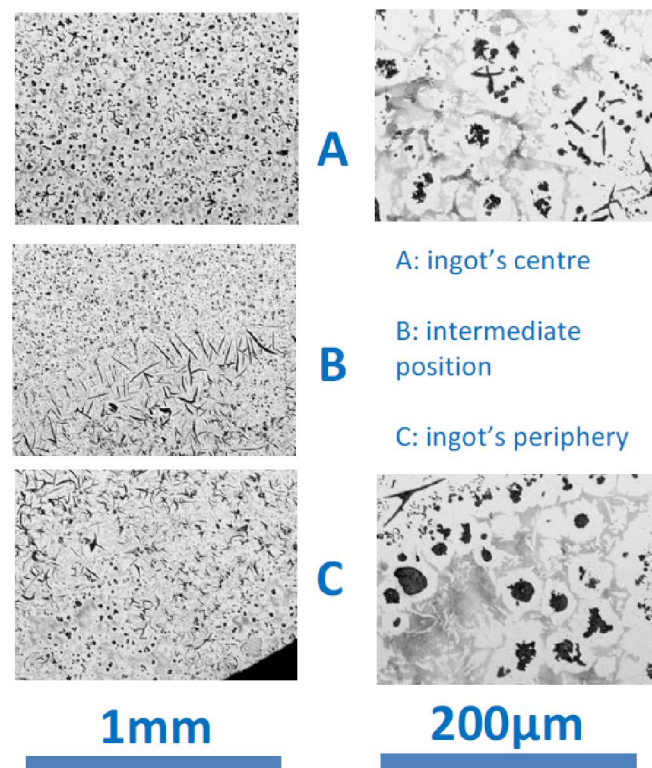


Figure 2 : Matrix structure (after Nital etching) of the "CoFe2" cast iron as observed at two magnifications in three distinct zones ("A", "B" and "C")

Full Paper

type (or hyper-eutectic?) microstructure (no visible dendrites), and clear tendency to spheroidal graphite in the ingot centre (zone A), however with significant quantities of flake graphite; in contrast coarse flake graphite near the ingot’s periphery (zone C); well-marked transition from coarse flake to compact/nodular in the intermediate zone (zone C)

After etching (Figure 2): grey areas far from the graphite phase and white areas close to the graphite particles (either lamellar or nodular)

“NiFe2” (Co=Fe + 3.5C + 2.5Si)

Before etching (Figure 3): very heterogeneous microstructure; more or less coarse flake graphite (including very fine graphite lamellae) in the ingot’s centre (zone A), extremely coarse flake graphite (and even plates) in the ingot’s periphery (zone C), seemingly transition in an intermediate zone (zone B), presence of small round graphite particles, and sometimes real graphite spheroids (Figure 4); no dendrites

After etching (Figure 4): no modifications

“FeFe2” (Co=Fe + 3.5C + 2.5Si)

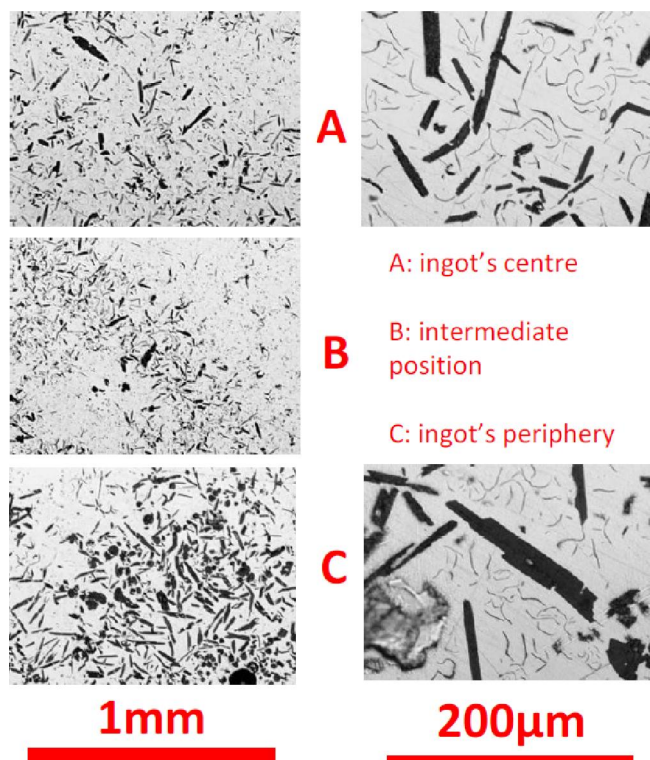


Figure 3 : Graphite structure (without etching) of the “NiFe2” cast iron as observed at two magnifications in three distinct zones (“A,” B” and “C”)

Before etching (Figure 5): very homogeneous microstructure, only graphite nodules

After etching (Figure 6): matrix made of grey

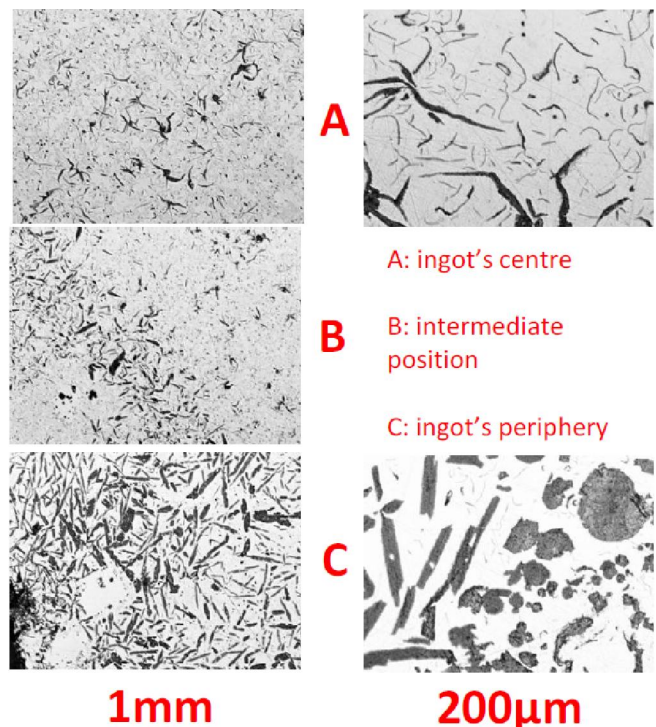


Figure 4 : Matrix structure (after Nital etching) of the “NiFe2” cast iron as observed at two magnifications in three distinct zones (“A,” B” and “C”)

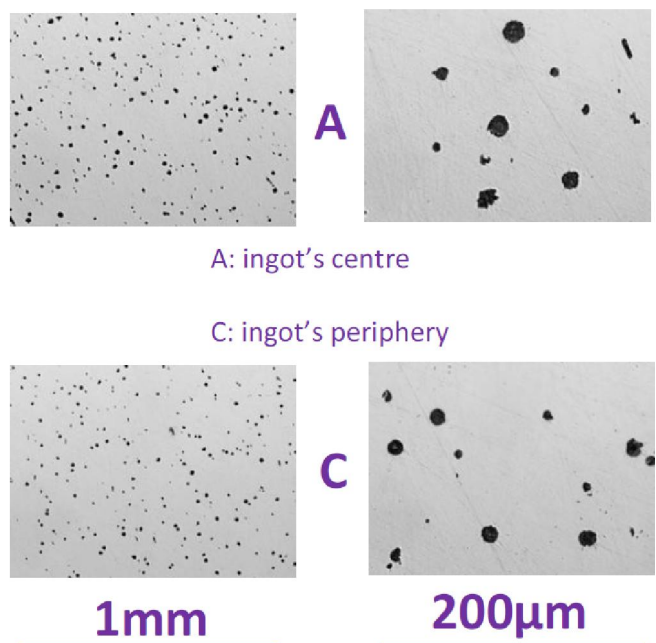


Figure 5 : Graphite structure (without etching) of the “FeFe2” cast iron as observed at two magnifications in three distinct zones (“A,” B” and “C”)

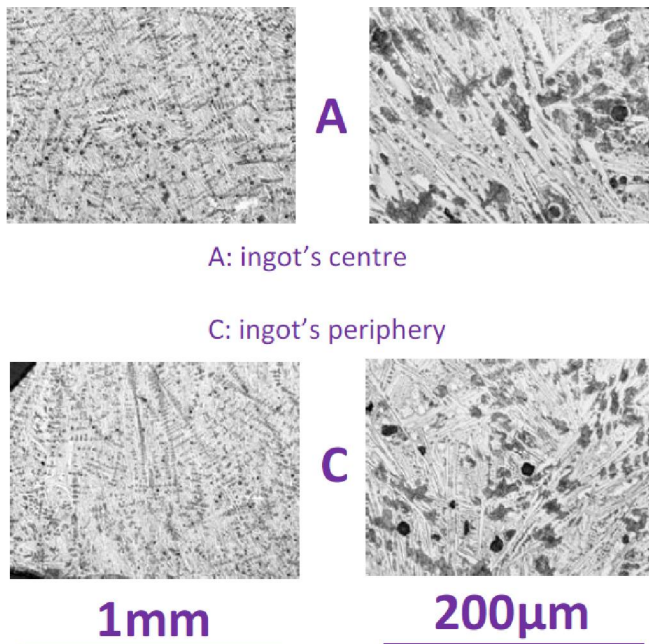


Figure 6 : Matrix structure (after Nital etching) of the “FeFe2” cast iron as observed at two magnifications in three distinct zones (“A,” “B” and “C”)

dendrites (austenite transformed in pearlite) and presence of cementite (in ledeburite)

Electronic microstructure observations

When observed with the SEM in Back Scattered

Electrons (BSE) mode, the microstructures are note really better visually characterized, as seen in Figure 7a for three locations in the “CoFe2” alloy, Figure 8a for the “NiFe2” alloy. Micrographs taken in Secondary Electrons (SE) mode at high magnification are displayed in Figure 7b for the “CoFe2” cast iron and in Figure 8b for the “NiFe2” one. This topological more of observation allows verifying that the black areas are not voids but really graphite, this being confirmed elsewhere by Energy Dispersion Spectrometry spot analysis showing qualitatively that the local carbon content is very high (more than 90 wt.% C).

The chemical compositions of the three samples were specified by full frame EDS analysis at $\times 250$ and by spot EDS analysis in the matrix for the “CoFe2” alloy and the “NiFe2” alloy (TABLE 1). Globally, the contents in Co and Fe in the “CoFe2” alloy (full frame or matrix) and in Ni and Fe in the “NiFe2” alloy are very similar to one another. The global Si contents (2.3-2.4 wt.% Si) are close to what was targeted, and the Si content in matrix is logically a little higher (2.6-2.8 wt.% Si).

XRD results

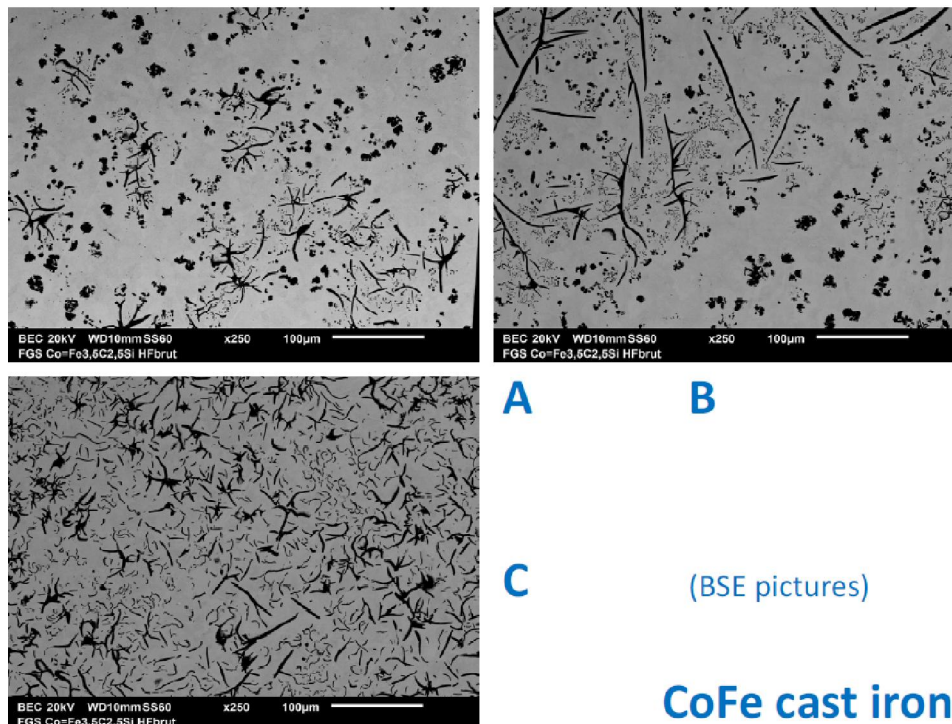


Figure 7a : Microstructure of the “CoFe2” cast iron as observed with the SEM (BSE mode) in three distinct zones (“A,” “B” and “C”)

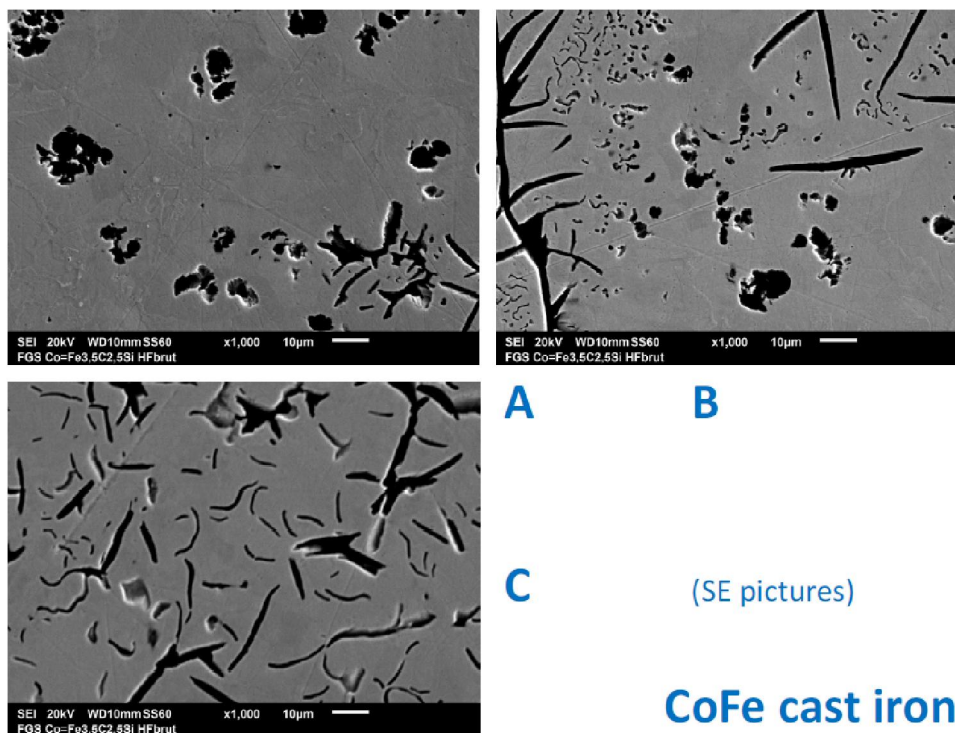


Figure 7b : Microstructure of the “CoFe2” cast iron as observed with the SEM (SE mode)at high magnification in three distinct zones (“A,” B” and “C”)

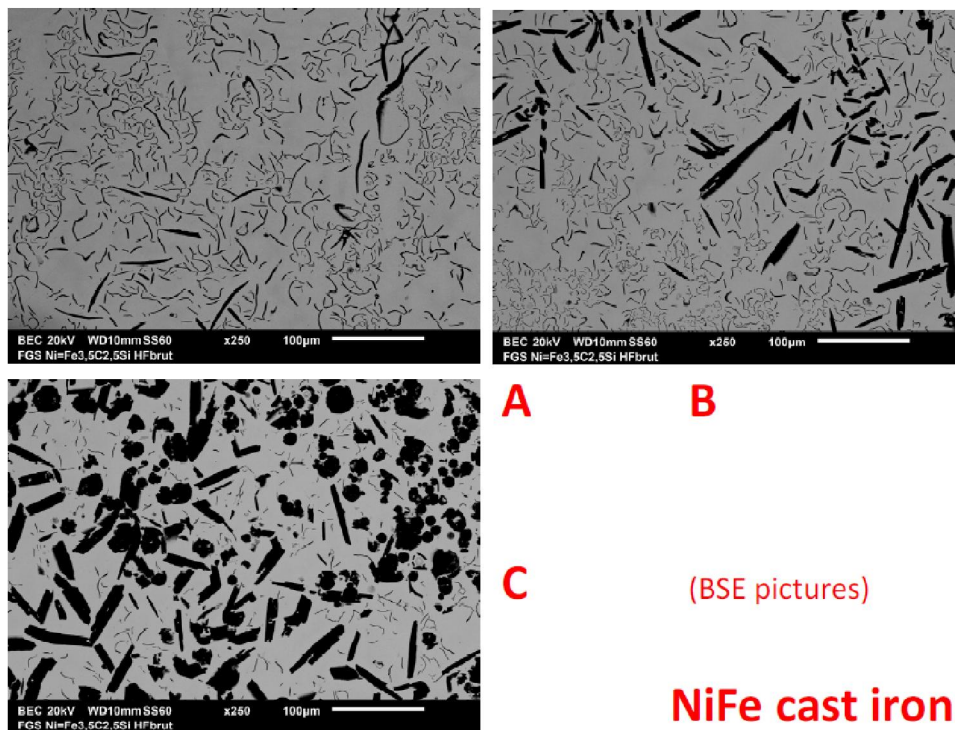
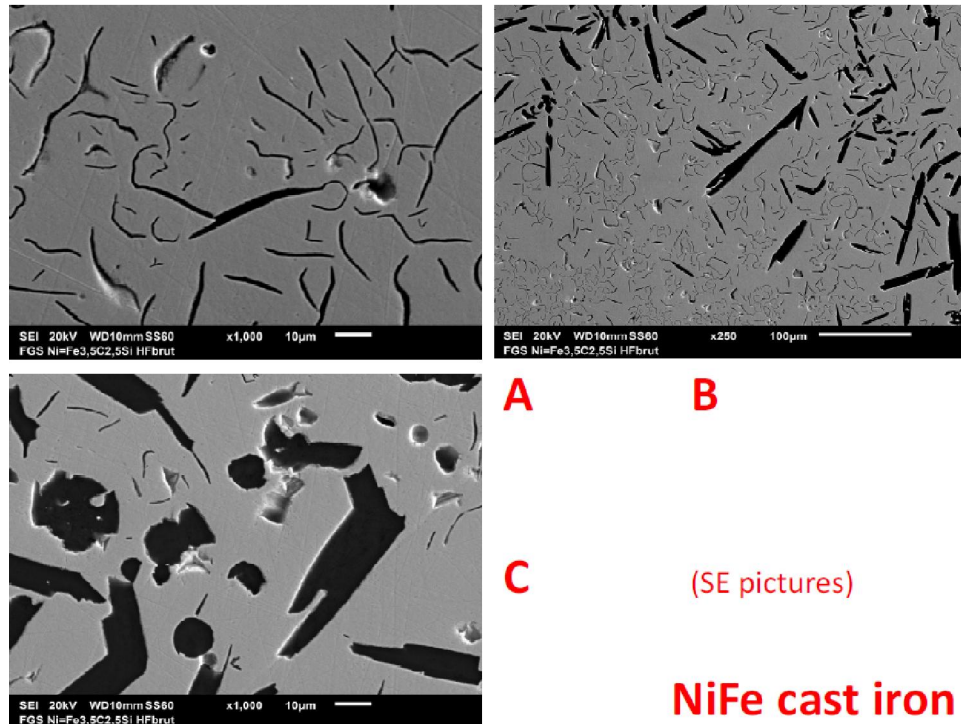


Figure 8a : Microstructure of the “NiFe2” cast iron as observed with the SEM (BSE mode) in three distinct zones (“A,” B” and “C”)

X-Ray Diffraction was performed on the three samples. The obtained diffractograms are presented in Figure 10 for the “CoFe” cast iron, in Figure 11

for the “NiFe” one and in Figure 12 for the “FeFe” one.

It seems that the matrix in the “CoFe” cast iron



A B
C (SE pictures)

NiFe cast iron

Figure 8b : Microstructure of the “NiFe2” cast iron as observed with the SEM (SE mode) at high magnification in three distinct zones (“A,” “B” and “C”)

TABLE 1 : Full frame (“GLOBAL”) and spot (“MATRIX”) EDS analysis results (from 3 to 7 results leading to an average value and a standard deviation one); carbon excluded (results automatically adjusted by the SEM to 100% without C)

"CoFe" GLOBAL			
Si	2.42	±	0.05
Fe	48.43	±	0.40
Co	48.62	±	0.27
Ni	0.52	±	0.14
wt.% (without C)			

"NiFe" GLOBAL			
Si	2.34	±	0.11
Fe	49.85	±	0.34
Co	nd	±	nd
Ni	47.81	±	0.23
wt.% (without C)			

"CoFe" MATRIX			
Si	2.59	±	0.20
Fe	50.20	±	3.24
Co	46.73	±	3.34
Ni	0.47	±	0.16
wt.% (without C)			

"NiFe" MATRIX			
Si	2.84	±	0.76
Fe	50.82	±	1.29
Co	0.23	±	0.22
Ni	46.25	±	1.84
wt.% (without C)			

(Figure 10) is essentially Body Centred Cubic (BCC), even if some peaks may correspond to a

Co_3Fe_7 cubic compound. Graphite seems to be detected too, as in the two other alloys. The “NiFe”

Full Paper

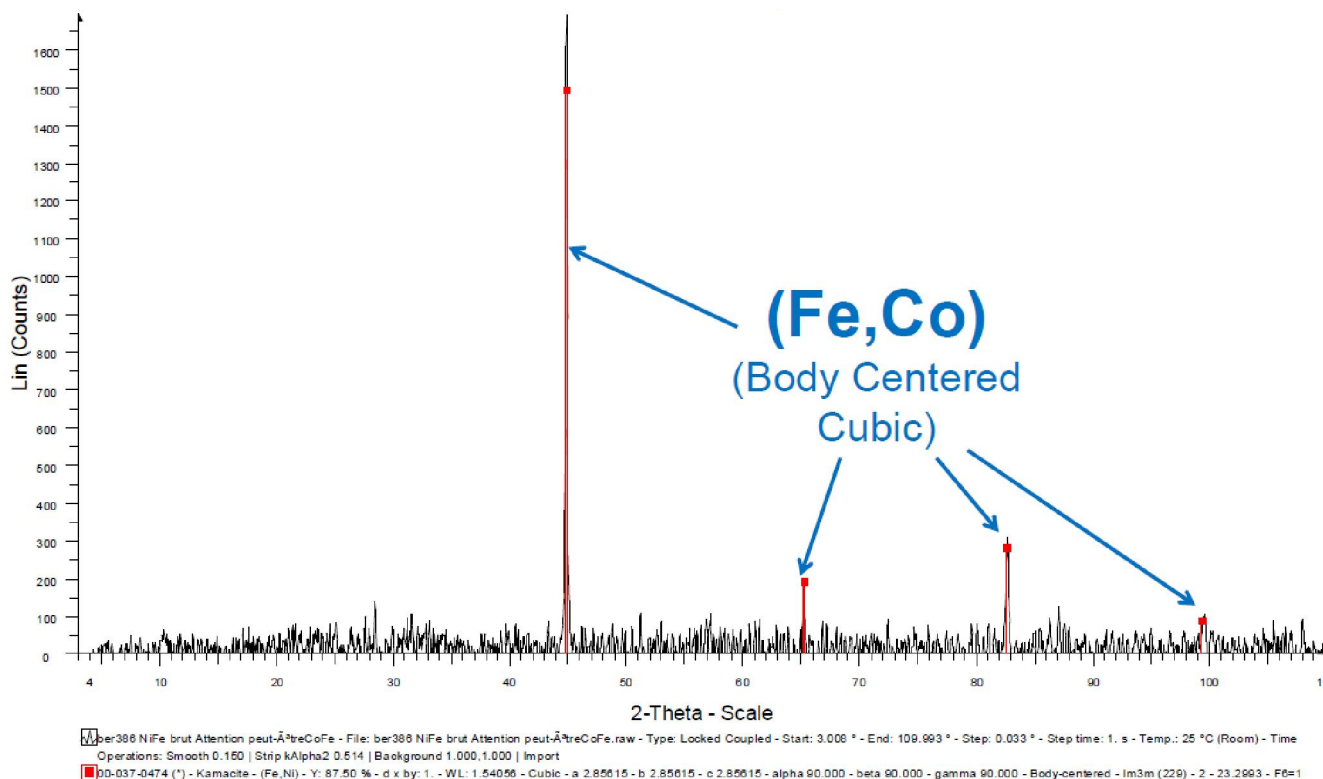


Figure 10 : X-Ray Diffractogram obtained on the “CoFe” cast iron

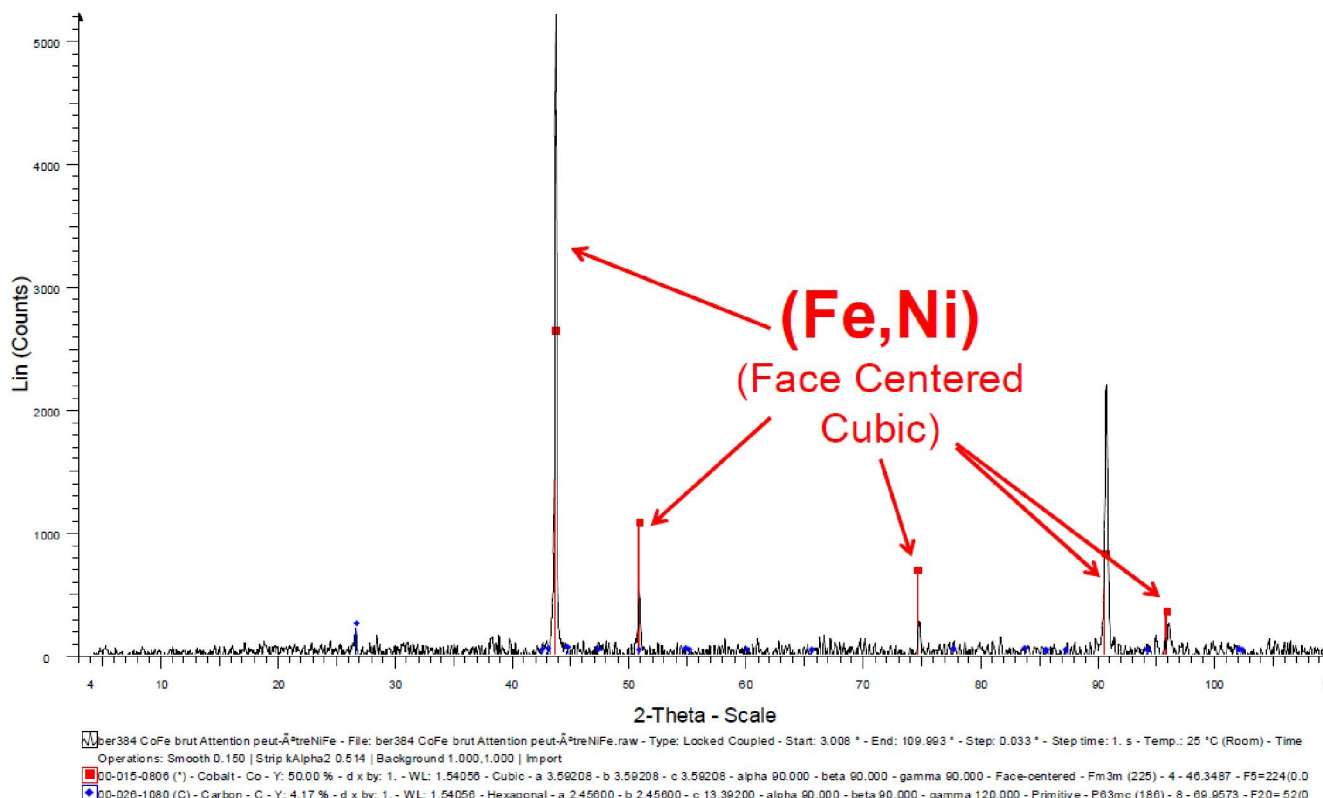


Figure 11 : X-Ray Diffractogram obtained on the “NiFe” cast iron

cast iron is essentially Face Centred Cubic (FCC) and the “FeFe” one logically BCC with also presence of cementite Fe_3C (orthorhombic).

General commentaries

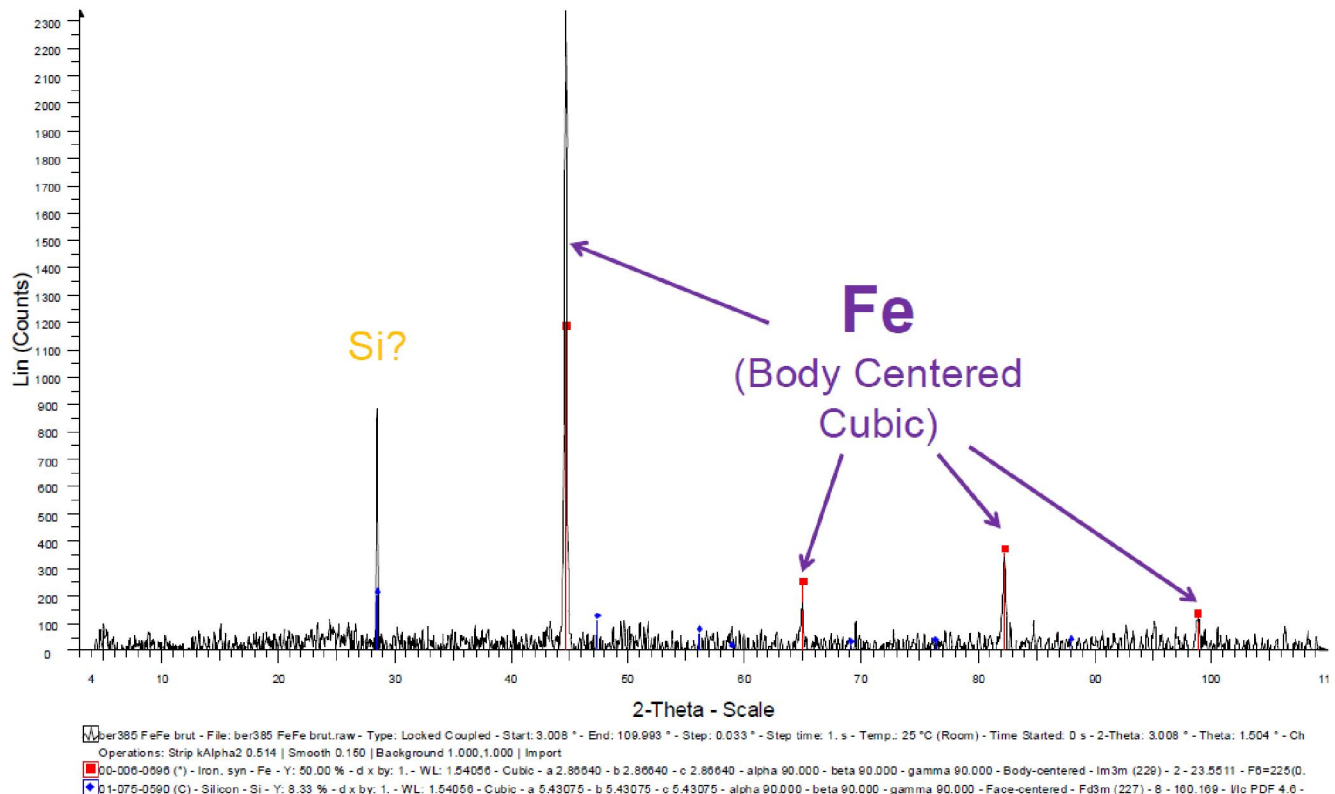


Figure 12 : X-ray diffractogram obtained on the “FeFe” cast iron

This new protocol, which allowed respecting the thermal cycle which previously permitted recovering the initial graphite nodules after re-melting for additional Si incorporation^[8,9], was thus totally successful. Indeed, the “FeFe2” cast iron was obtained with only nodular graphite. This permits affirming that the perfectible nodular graphite obtained in the “CoFe2” cast iron may be due to the fact that this is not Fe but Co which was added, as is to say cobalt may tend to be unfavorable to the spheroidal crystallization of graphite. This is worse with nickel since the obtained graphite particles were essentially flake/lamellar and even plate-like. Since it was thought that the used nickel was may be not pure enough (and maybe contained a little but too high level of sulfur) a new elaboration of a “NiFe2” cast iron was additionally carried out following this new protocol, but using ultra-pure Ni. No improvement of the graphite shape was obtained: still almost no nodules.

Concerning the matrix, the semi-SG “CoFe2” cast iron seems to be essentially ferritic (BCC) as the flake graphite “CoFe” one^[10]. The dark-colored areas situated far from graphite appeared after Nital

etching are similar to the ones previously observed in the etched “CoFe” cast iron: they remain to be clearly identified, by other means than SEM/EDS and XRD (deeper investigations can be done by microprobe). The “NiFe2” did not react with Nital, this demonstrating a probable good corrosion resistance, useful for avoiding the presence of chromium which may threaten ductility and toughness because being a strong carbide-forming element. The “FeFe2” cast iron, the graphite of which is really spheroidal, seems richer in carbides than the flake graphite “FeFe” cast iron previously obtained. The slower nucleation and growth of the eutectic spheres are probably responsible of a greater part of solidification realized in the metastable Fe-C system.

CONCLUSION

Thus it appeared possible but rather difficult to obtain {Co=Fe}-based spheroidal graphite cast iron by re-melting an initial SG iron to incorporate high amount in cobalt. In the case of nickel it seems more difficult again. However curious and interesting graphite morphologies (coarse plates instead nodu-

Full Paper

lar or lamellar graphite) were obtained. A progress was nevertheless realized with this new protocol, with results clearly showing that overheating is to be avoided to keep chance of recovering totally ("FeFe2" cast iron) or at least a part ("CoFe2" cast iron) of the initial spheroids. After having characterized the microstructures of these new highly Co-alloyed and Ni-alloyed cast irons, their mechanical properties will be studied by compression tests and indentation^[11].

ACKNOWLEDGEMENTS

The authors wish to thank Pascal Villeger who performed the X-Ray Diffraction runs.

REFERENCES

- [1] J.Szekely; Blast furnace technology, Science and Practice, Dekker, (1972).
- [2] J.Szekely, J.W.Evans, H.Y.Sohn; Gas-Solid Reactions, Academic Press Inc., New York, (1976).
- [3] G.Béranger; Le livre de l'acier, Lavoisier, Paris Cachan, (1994).
- [4] J.R.Davis; Cast Irons, ASM International, (1996).
- [5] M.Durand-Charre; La Microstructure des aciers et des fontes, Genèse et interprétation, SIRPE, Paris, (2003).
- [6] M.Durand-Charre; Microstructure of steels and cast irons – engineering materials and processes, Springer-Verlag, Berlin Heidelberg New York, (2004).
- [7] G.Lesoult; Traité des matériaux: Tome 5, Thermodynamique des matériaux : De l'élaboration des matériaux à la genèse des microstructures, Presses Polytechniques et Universitaires Romandes, (2010).
- [8] S.Diallo; Détermination du comportement en oxydation des fontes à haute température, report of Master 2 Chemistry of Solids trainee period, Université de Lorraine, (2014).
- [9] S.Diallo, P.Berthod; Materials Science : An Indian Journal, **12(8)**, 277 (2015).
- [10] K.Meridja, P.Berthod, E.Conrath; Materials Science: An Indian Journal, *submitted*.
- [11] K.Meridja, P.Berthod; Materials Science: An Indian Journal, *to be submitted*.